

Supporting Information for

Energy Level Alignment at Hybridized Organic-Metal Interfaces: The Role of Many-Electron Effects

Yifeng Chen¹, Isaac Tamblyn^{2,3} and Su Ying Quek^{1,4*}

¹Centre for Advanced 2D Materials and Graphene Research Centre, National University of Singapore, 6 Science Drive 2, Singapore 117542

²National Research Council of Canada, 100 Sussex Drive, Ottawa, Ontario, K1A 0R6, Canada

³Department of Physics, University of Ontario Institute of Technology, Oshawa, Ontario, L1H 7K4

⁴Department of Physics, National University of Singapore, 2 Science Drive 3, Singapore 117551

*: Corresponding author: phyqsy@nus.edu.sg

Table of contents

- 1) General details on computational methods used**
- 2) Details of molecular GW self-energy projection calculation**
- 3) GW convergence of Au(111) work function**
- 4) GW convergence of gas-phase molecular orbital levels**
- 5) Off-diagonal elements of GW self-energy evaluated in the BDA MO basis for Geometry 4**
- 6) Off-diagonal elements of GW self-energy evaluated in the BP MO basis for Geometry 7**
- 7) Off-diagonal elements of GW self-energy evaluated in the BT MO basis for Geometry 11**
- 8) Other geometries considered for BDA molecular layer on Au(111)**
- 9) Geometries of metal/molecule/metal junction structures**
- 10) Decomposed self-energy contributions of MO levels from GW versus static-COHSEX results: Comprehensive result**
- 11) Charge rearrangement and binding energy upon molecular adsorption on the Au(111) surface**

- 12) Molecule/metal slab geometric parameters**
- 13) DFT and GW bandstructure for the BDA layer as in Geo. 4**
- 14) GW projected molecular level dispersion across the Brillouin zone**
- 15) Calculated image charge correction energy for the hybridized slabs**
- 16) Projected density of states together with our DFT starting points marked for Geo.'s 1-11 investigated in this work.**
- 17) Table S11 summarizing all data**

1) General details on computational methods used

Geometry optimization was performed using both VASP [1] and Quantum-ESPRESSO [2] (Q.E.). To account for long-range van der Waals interactions, we used both the Grimme's PBE-D2 method [3] (as implemented in Quantum Espresso) and the van der Waals density functional (vdW-DF2, optB86b) [4,5] (as implemented in VASP); key geometric parameters are given in Table S8 for all geometries in this work. Geometry 3 was built from experimental information [6] and relaxed in VASP with vdW-DF2 (optB86b), while the BDA linear chain model was provided by Guo Li [7]. Bader charge analysis was performed on total charge densities produced by Q.E. with the UTexas code [8].

GW calculations were done using the BerkeleyGW package [9], with DFT wavefunction input taken from Q.E. using a norm-conserving pseudopotential, PBE exchange-correlation functional, 60 Ry kinetic energy cutoff, and 10^{-6} Ry convergence threshold. Due to the spatial overlap of semi-core and valence wavefunctions in Au [10], we used a 19-electron Au pseudopotential in our GW calculations. A vacuum size of at least 13 Å between periodic slabs was used, and the Coulomb interactions between supercells were truncated with the “cell_slab truncation” and “cell_box truncation” methods. We employed a 20 Ry energy cutoff for the epsilon matrix (epsilon cutoff), as well as a 20 Ry screened Coulomb cutoff. We used 5000 bands for $15 \times 15 \times 15$ Å³ cells and the equivalent number in other cells (scaled according to volume). For $\sqrt{3} \times \sqrt{3}$ R30° cells we use a 3x3x1 Monkhorst-Pack k-mesh, while for 3x3 cells we use a 2x2x1 k-mesh. The $\mathbf{q} \rightarrow 0$ limit for metallic slabs was treated using a wavefunction with twice as dense a k-mesh but fewer unoccupied states. The static remainder method was used to help with convergence of the self-energy [11].

We performed one-shot GW calculations using a projection approach. To do this, we obtain the DFT converged wavefunction for both the slab ($|\Psi_{slab}\rangle$) and the isolated molecule in the same geometry as in the slab ($|\varphi_{mol}\rangle$). The slab wavefunction is used to construct the dielectric matrix ϵ and the self-energy operator $\Sigma(E)$ as in normal GW calculations, but in the sigma output step, we utilize the WFN_outer facility that comes with the BerkeleyGW package [9], to evaluate the self-energy expectation values within the molecular wavefunction basis as in Eq. 1. More details are given in Section 2.

The image charge model used here is similar to Ref. [12]. The image plane position is taken to be 0.9 Å above the Au(111) surface [13]. The molecular orbital charge distribution was obtained using SIESTA [14] calculations of gas-phase molecules with the same geometry as their corresponding hybrid slabs, and mulliken populations at each atom are used to compute the image charge energy. For thiolate/Au systems, the molecular orbital distribution was obtained by passivating the thiolate group with the cleaved hydrogen atom. For molecules with metal contacts on both sides, a Mathematica worksheet was used to take into account infinite number of images. Visualization of all geometries in this work was achieved by the XCrysDen software [15].

2) Details of molecular GW self-energy projection calculation

In order to evaluate the self energy in the basis of the orbitals of the isolated molecule, the eqp_outer_corrections flag must be used in the sigma input file in BerkeleyGW.

When this flag is set, the sigma executable will look for WFN_outer, the wavefunctions used for evaluating the self-energy correction. WFN_outer will be the wavefunctions of the isolated molecule in this case.

Also, the sigma executable will look for eqp_outer.dat, that contains the DFT starting points for the eigenvalues, as well as the corrected energies at which the self energy is to be evaluated. We run sigma twice. In the first run, eqp_outer.dat contains the DFT levels of the molecular orbital peaks in the slab calculation (this is described below). The corrected energies are also set to be the same as these DFT starting levels. The sigma run will then generate a new eqp_outer.dat which replaces the corrected energies with the computed quasiparticle energies. Sigma is then run a second time, reading this new eqp_outer.dat. In this run, we should see in the output that eqp1 (the final quasiparticle value) is very close to ecor (the energy value read in from eqp_outer.dat, at which the sigma operator is evaluated).

The above will ensure that we are evaluating sigma using the molecular wavefunctions, and that the energies at which we are to evaluate sigma are not those of the isolated molecule, but are those of the molecular peaks in the slab calculation. We also need to make sure that the mean-field exchange-correlation term is computed using the molecular wavefunctions and not the slab wavefunctions. To do so, we do not copy vxc.dat (the

matrix elements of the exchange-correlation potential) into the sigma folder but copy the exchange-correlation potential file VXC instead. This will make the sigma executable compute the required matrix elements from the exchange-correlation potential file VXC with the new WFN_outer wavefunctions basis.

For the above to work, the BerkeleyGW code (Version 1.0.6) needs a few minor modifications. Firstly, BerkeleyGW will automatically check that the WFN_outer headings are the same as the WFN_inner headings. This check needs to be removed. Secondly, a new routine must be added to read the DFT starting levels (elda in the sigma output) from eqp_outer.dat, as explained above.

To get the initial DFT eigenvalue starting levels for the eqp_outer.dat file, we utilize the wavefunction projection utility wfn_dotproduct.x that comes with BerkeleyGW. The projection is done at Γ -point only, which outputs the squared modulus overlap weights of i-th molecular level upon all the hybrid slab wavefunction basis manifold and sums up to 1:

$$w_J^i = |\langle \varphi_{mol}^i | \Psi_{slab}^J \rangle|^2, \quad \sum_{J=1}^{N_{slab}} w_J^i = 1. \quad (\text{S1})$$

By plotting the weights distribution of one particular MO level across the energy axis, we can readily identify an appropriate DFT energy point for this molecular state taken at the highest weighting factor point. In some cases, the MO can have weights scattered across a large energy range without any particular prominent peaks, which we take as spectroscopically undefined. The comparison of these DFT starting points with DFT molecular projected density of states (PDOS) plot reveals that they correspondingly according to respective molecular peaks in DFT PDOS.

3) GW convergence of Au(111) work function

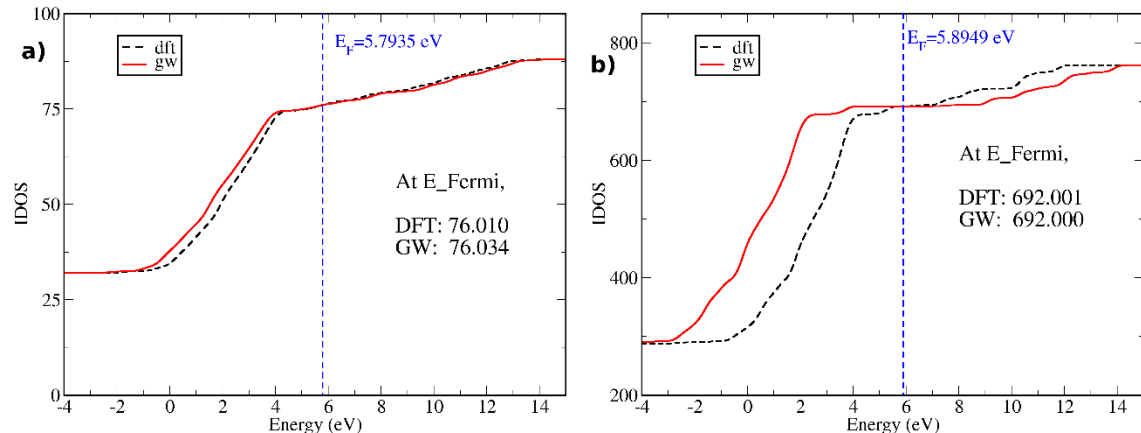


Figure S1. (a) Integrated density of states (IDOS) of Au(111) from GW and DFT PBE. DFT PBE predicts an accurate work function for Au(111) (5.3 eV). So if the IDOS from GW and PBE match well at the DFT Fermi level, GW will also give the same Fermi level, hence the same metal work function. Calculation details: 1x1 cell, 4 layer Au(111) slab cell with the 19e⁻ PBE norm-conserving Au pseudopotential optimized lattice constant at 8.06 Bohr, 13 Å vacuum space, 20 Ry epsilon cutoff and screened Coulomb cutoff, 60 Ry bare Coulomb cutoff, K-mesh/q-mesh 6x6x1, fine mesh 12x12x1 for approaching the $\mathbf{q} \rightarrow 0$ limit, slab Coulomb truncation. (b) Similar to a) but using the Wigner-Seitz box Coulomb truncation method on the 3x3 Au(111) cell with 4 layers of gold, calculated at the Γ point only. It is seen that this truncation does not affect the precision of our GW work function prediction.

Table S1: Comparison of results from different treatment of the $\mathbf{q} \rightarrow 0$ limit for bare Au(111) system as well as in Geo. 3. For the Au(111) cell, we compare the difference between GW Fermi level and DFT Fermi level, i.e. $E_F^{\text{GW}} - E_F^{\text{DFT}}$; for Geo. 3, we compare the difference between GW HOMO level and DFT Fermi level, i.e. $E_{\text{HOMO}}^{\text{GW}} - E_F^{\text{DFT}}$. We see that the change in the GW HOMO level for different treatments of the $\mathbf{q} \rightarrow 0$ limit was completely due to a corresponding GW Fermi level shift in an equivalent treatment of the $\mathbf{q} \rightarrow 0$ limit for the Au(111) slab. Different fine meshes are used to approach the $\mathbf{q} \rightarrow 0$ limit. With no Coulomb truncation, an averaging procedure is done in a region of the Brillouin Zone near $\mathbf{q} = 0$. It is important to note that the reference Fermi level of the GW spectrum has to be carefully calibrated against the DFT Fermi level. Otherwise, a rigid shift of the whole spectrum might result in incorrect level alignment predictions.

Au(111) 1x1 cell, 4 layer slab	$E_F^{\text{GW}} - E_F^{\text{DFT}}$ (eV)	Geo. 3, 3x3 Au(111) cell with BDA	$E_{\text{HOMO}}^{\text{GW}} - E_F^{\text{DFT}}$ (eV)
6x6x1 q-mesh, 12x12x1 fine-mesh, w/ slab truncation	0		-1.30
6x6x1 q-mesh, 18x18x1 fine-mesh, w/ slab truncation	-0.37		-1.66
6x6x1 q-mesh, 12x12x1 fine-mesh, no Coulomb truncation	-0.65		-1.98

4) GW convergence of gas-phase molecular orbital levels

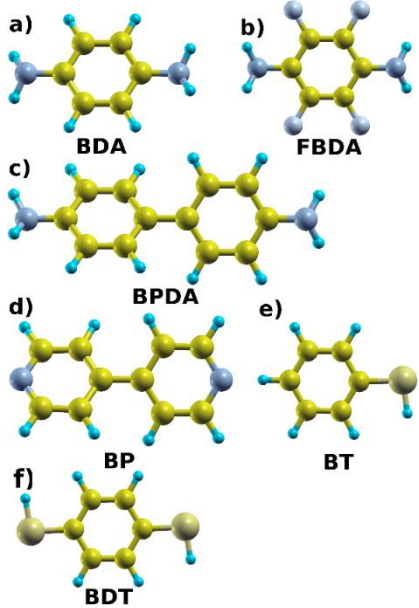


Figure S2: Molecules investigated in this work. BDA: BenzeneDiAmine; FBDA: Fluorinated BenzeneDiAmine; BPDA: BiPhenylDiAmine; BP: BiPyridine; BT: BenzeneThiol; BDT: BenzeneDiThiol.

Table S2: Converged GW results for the studied gas-phase single molecules. ΔE 's refer to GW correction upon their DFT corresponding levels. $E_{\text{gap}} = \text{IP} - \text{EA}$. Energy units are in eV. We note that the numbers reported here are obtained using a 24 Ry epsilon cutoff, 5000 bands for $15 \times 15 \times 15 \text{ \AA}^3$ cells (following previous literature [16]), and a box Coulomb truncation scheme [9]. However, similar to Ref. [16], we obtain essentially the same results with a 20 Ry epsilon cutoff, which is used in our slab calculations.

	IP(G_0W_0)	EA(G_0W_0)	$\Delta E(\text{HOMO})$	$\Delta E(\text{LUMO})$	$E_{\text{gap}}(G_0W_0)$
BDA	7.16	-1.01	-2.91	+2.04	8.17
FBDA	7.85	-0.37	-2.97	+1.90	8.22
BPDA	6.95	-0.48	-2.53	+1.65	7.43
BP	9.32	+0.99	-3.27	+1.89	8.33
BT	8.73	-0.50	-3.15	+2.08	9.22
BDT	7.91	-0.38	-2.64	+2.28	8.29

5) Off-diagonal elements of GW self-energy evaluated in the BDA MO basis for Geometry 4

Table S3: Off-diagonal elements of GW self-energy evaluated in the BDA MO basis for Geometry 4. Only MOs close to the frontier orbitals are considered, as orbitals further away have even smaller probability of mixing with the frontier MOs. Results are shown for both the slab and box truncation schemes. The self-energy for each entry is evaluated at the energy corresponding to the MO identified by the row index of the entry.

Slab GW	HOMO-1	HOMO	LUMO	LUMO+1
HOMO-1	-13.8720	-0.0052 -i*0.0021	0.0003+i*0.0074	-0.0003 +i*0.0002
HOMO	-0.0052 +i*0.0020	-15.3778	-0.0013-i*0.0548	0.0514 -i*0.0243
LUMO	-0.0002- i*0.0112	-0.0005 +i*0.0552	-10.2048	-0.1436 +i*0.0675
LUMO+1	-0.0003- i*0.0002	0.0481+i*0.0228	-0.1443-i*0.0678	-4.3570
<hr/>				
Box GW	HOMO-1	HOMO	LUMO	LUMO+1
HOMO-1	-15.9543	0.0002-i*0.0009	-0.0014 +i*0.0136	0.0000- i*0.0000
HOMO	0.0002 +i*0.0009	-17.4108	-0.0019 -i*0.0000	0.0924- i*0.0432
LUMO	-0.0027- i*0.0226	-0.0018 +i*0.0000	-10.2060	-0.1349 +i*0.0628
LUMO+1	0.0001 -i*0.0002	0.0888 +i*0.0416	-0.1356 -i*0.0632	-4.6174

6) Off-diagonal elements of GW self-energy evaluated in the BP MO basis for Geometry 7

Table S4: Off-diagonal elements of GW self-energy evaluated in the BP MO basis for Geometry 7. Note that HOMO level at the interface is not well-defined here. Other details follow those in Table S3.

Slab GW	HOMO-1	LUMO	LUMO+1
HOMO-1	-17.7891	-0.0034-i*0.0095	0.0919-i*0.0428
LUMO	-0.0032+i*0.0095	-13.7422	-0.0005-i*0.0041
LUMO+1	0.0922+i*0.0430	-0.0005+i*0.0041	-10.6064
<hr/>			
Box GW	HOMO-1	LUMO	LUMO+1
HOMO-1	-20.0532	-0.0007+i*0.0001	0.0874-i*0.0409
LUMO	-0.0007-i*0.0001	-16.0462	-0.0001+i*0.0001
LUMO+1	0.0876+i*0.0411	-0.0001-i*0.0000	-10.3741

7) Off-diagonal elements of GW self-energy evaluated in the BT MO basis for Geometry 11

Table S5: Off-diagonal elements of GW self-energy evaluated in the BT MO basis for Geometry 11. Note that HOMO level at the interface is not well-defined here. Other details follow those in Table S3.

Slab GW	HOMO-1	HOMO	LUMO	LUMO+1
HOMO-1	-13.8048	-0.0060 -i*0.0048	0.0190 -i*0.0057	0.0048 +i*0.0125
HOMO	-0.0060 +i*0.0049	-13.7622	0.0241 -i*0.0441	0.5737 +i*0.3368
LUMO	0.0172 +i*0.0051	0.0241 +i*0.0441	-10.4989	0.0018 -i*0.0679
LUMO+1	0.0053 -i*0.0137	0.5831 -i*0.3423	0.0018 +i*0.0678	-11.1179
<hr/>				
Box GW	HOMO-1	HOMO	LUMO	LUMO+1
HOMO-1	-15.8129	-0.0063 -i*0.0050	0.0220 -i*0.0103	0.0050 +i*0.0141
HOMO	-0.0063 +i*0.0051	-15.8501	0.0240 -i*0.0434	0.6618 +i*0.3916
LUMO	0.0084 +i*0.0051	0.0239 +i*0.0432	-10.5077	0.0022 -i*0.0805
LUMO+1	0.0061 -i*0.0170	0.6696 -i*0.3963	0.0022 +i*0.0805	-11.2050

8) Other geometries considered for BDA molecular layer on Au(111)

The geometry used in Reference [6] was a face-on configuration in a 4x4 Au(111) cell, relaxed using DFT PBE without including van der Waals interactions. We have performed a geometry optimization of the same system using the vdW-DF2 functional and found that this coverage is likely to be too low (Figure S3). Geometry optimization using the vdW-DF2 functional found that the benzene ring is tilted 18.2° from the surface. Similar geometry optimization for the 3x3 Au(111) cell found a corresponding tilt angle of 24°, which is closer to the experimentally determined angle of 24°±10°. We also see that the amine group further from the surface is tilted toward the surface, away from the plane of the phenyl ring, by about 8°. This suggests that lower coverages would result in smaller tilt angles further from the experimental value, which is defined for “monolayer coverage” [6].

The geometry used in Reference [7] was a linear chain motif of BDA molecules on Au(111), which was experimentally observed at low temperature [17]. Using this same structure, we found a GW HOMO level of -0.75 eV and a DFT+ Σ HOMO level of -2.58 eV (including the 0.3 eV intra-layer polarization as in Ref. [7]). The fact that GW predicts a HOMO level much closer to E_F than the UPS value indicates that the linear chain geometry, which is stabilized by hydrogen bonds at 5 K [17], is not an appropriate geometry for the room temperature UPS experiment [6].

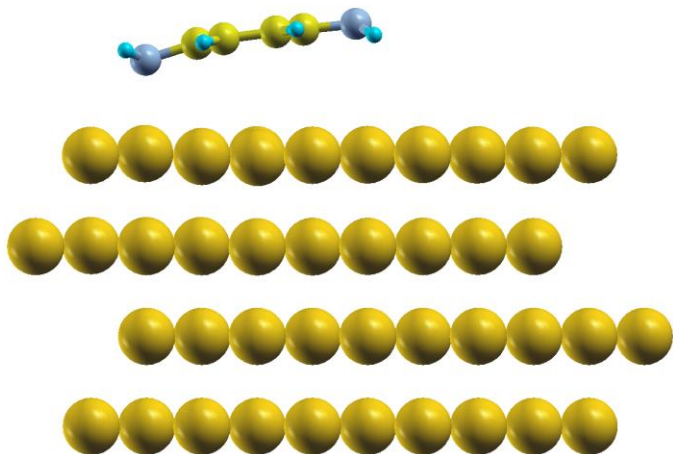


Figure S3. Optimized geometry of BDA in a 4x4 Au(111) cell in the face-on geometry (VASP, vdW-DF2 functional).

9) Geometries of metal/molecule/metal junction structures

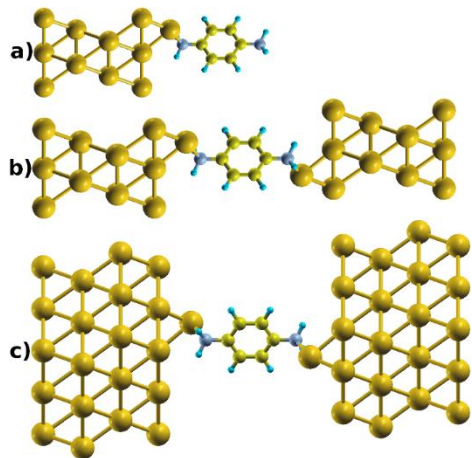


Figure S4. a) BDA vertical up-right geometry in $\sqrt{3}\times\sqrt{3}$ R30° Au(111) cell; b) Au(111)/BDA/Au(111) junction structure with $\sqrt{3}\times\sqrt{3}$ R30° cell; c) Au(111)/BDA/Au(111) junction structure with 3x3cell.

10) Decomposed self-energy contributions of MO levels from GW versus static-COHSEX results: Comprehensive result

Table S6: Components of the GW and static COHSEX self-energy corrections for different geometries, together with the bare exchange term (X). SX is screened exchange, CH the Coulomb hole term. The GW self-energy is equal to difference between (SX+CH) and the mean-field exchange-correlation term. The X term is given for comparison. Units are in eV. The red, blue and green colors are used as a guide to the eye for the discussion in the main text.

	Method	X	SX	CH
BDA HOMO in Geo. 2	Slab GW	-16.096	-7.474	-7.910
	Slab static-COHSEX	-16.096	-7.384	-9.171
	Box GW	-17.736	-9.267	-7.957
	Box static-COHSEX	-17.736	-9.266	-9.689
BDA HOMO in Geo. 4	Slab GW	-15.904	-7.286	-8.033
	Slab static-COHSEX	-15.904	-7.162	-9.356
	Box GW	-17.474	-9.158	-7.923
	Box static-COHSEX	-17.474	-9.092	-9.680
BDA LUMO in Geo. 4	Slab GW	-7.434	-3.270	-7.170
	Slab static-COHSEX	-7.434	-3.471	-7.802
	Box GW	-7.444	-3.078	-7.356
	Box static-COHSEX	-7.444	-3.304	-8.115
F4BDA HOMO in Geo. 5	Slab GW	-16.753	-8.094	-8.068
	Slab static-COHSEX	-16.753	-8.048	-9.355
	Box GW	-18.440	-9.897	-8.058
	Box static-COHSEX	-18.440	-9.857	-9.793
BPDA HOMO in Geo. 6	Slab GW	-15.054	-7.323	-7.600
	Slab static-COHSEX	-15.054	-7.376	-8.806
	Box GW	-16.754	-9.027	-7.662

	Box static-COHSEX	-16.754	-9.041	-9.373
BP HOMO-1 in Geo. 7	Slab GW	-20.019	-9.647	-7.976
	Slab static-COHSEX	-20.019	-9.543	-9.488
	Box GW	-21.603	-11.624	-7.878
	Box static-COHSEX	-21.603	-11.597	-9.846
BP LUMO in Geo. 7	Slab GW	-13.810	-5.388	-8.388
	Slab static-COHSEX	-13.810	-5.200	-9.548
	Box GW	-9.677	-3.990	-8.500
	Box static-COHSEX	-9.677	-4.221	-9.438
BT HOMO in Geo. 8	Slab GW	-13.877	-5.365	-8.159
	Slab static-COHSEX	-13.877	-4.960	-9.566
	Box GW	-15.105	-7.214	-7.813
	Box static-COHSEX	-15.105	-6.898	-9.564
BT HOMO in Geo. 9	Slab GW	-13.652	-4.475	-8.536
	Slab static-COHSEX	-13.652	-4.089	-9.921
	Box GW	-15.451	-7.621	-7.594
	Box static-COHSEX	-15.451	-7.534	-9.301
BT LUMO in Geo. 9	Slab GW	-7.422	-3.177	-7.730
	Slab static-COHSEX	-7.422	-3.408	-8.518
	Box GW	-7.448	-3.061	-7.538
	Box static-COHSEX	-7.448	-3.323	-8.297

11) Charge rearrangement and binding energy upon molecular adsorption on the Au(111) surface

Table S7: Number of electrons lost by the molecule (mol.) or the anchoring atom (N for amine and pyridine, S for thiol), and binding energy upon adsorption of the molecule on the Au(111) surface. The desorbed hydrogen atom from thiol is taken to carry a charge of 1 electron, and is taken into consideration in the final result below. (Geo.: Geometry)
There is little net charge transfer from the molecule to the metal, but for thiols, there is significant local charge rearrangement in the molecule. The binding energy is computed as the difference in energy between the hybrid system and the sum of the energies of the gas phase molecule/radical and the Au surface.

	Geo. 1	Geo. 2	Geo. 3	Geo. 4	Geo. 5	Geo. 6	Geo. 7	Geo. 8	Geo. 9	Geo. 10
Mol.	0.086	0.182	0.159	0.193	0.142	0.177	0.048	-0.117	-0.167	-0.132
Anchor	-0.019	-0.449	-0.385	0.144	0.106	0.117	0.158	-1.307	-1.411	-1.457
Binding energy (eV)	-0.772	-1.502	-1.615	-1.083	-0.902	-1.023	-1.099	-2.217	-1.036	-0.999
	Geo. 4 @6L Au		Geo. 4 @4x4 Au		Geo. 9 @6L Au		Geo. 10 @6L Au		Geo. 11	
Mol.	0.197		0.227		-0.152		-0.107		-0.078	
Anchor	0.129		0.159		-1.484		-1.442		-1.334	
Binding energy (eV)	-1.091		-1.123		-		-		-2.189	

12) Molecule/metal slab geometric parameters

Table S8: Summary of geometric parameters for Geometries **1** to **11**

	Au-N(S) bond length (Å)	Au-N-C (Au-S-C) bond angle (°)
Geo. 1	2.609	136.86
Geo. 2	2.359	119.87
Geo. 3	2.448	112.5
Geo. 4	2.338	114.0
Geo. 5	2.338	114.0
Geo. 6	2.338	114.2
Geo. 7	2.154	120.0
Geo. 8	2.279	105.74
Geo. 9	2.270	179.90
Geo. 10	2.276	179.82
Geo. 11	2.489	132.058

Atomic geometric coordinates of BDA/Au systems from Geo. **1** to Geo. **4** are also listed below. Coordinates for Geo. **5 ~ 11** are listed at the end of this document after the Reference section.

XYZ format coordinates for Geo. **1**:

28

BDA/Au111 geo. 1

C	3.140518	1.457933	10.954336
C	4.460963	1.453559	13.472880
C	4.142933	2.650504	12.819166
C	3.523252	0.261119	11.567874
C	3.525667	2.652449	11.570825
C	4.140521	0.258851	12.816215
H	4.389917	3.604348	13.289313
H	3.274155	-0.689438	11.092153
H	3.278212	3.604650	11.097572
H	4.385838	-0.696546	13.284024
H	1.793448	2.298496	9.648112
H	5.549743	0.610949	14.995625
H	1.786475	0.626477	9.649273
H	5.551583	2.289944	14.997831
N	2.363610	1.460196	9.778419
N	5.026047	1.451323	14.757731
Au	0.240047	-0.004960	7.177793
Au	2.802509	1.455866	7.206997
Au	5.283109	2.917041	7.177696
Au	1.808581	0.009923	4.762676
Au	1.808580	2.901915	4.762701
Au	4.312146	1.455923	4.762151
Au	0.840531	1.455842	2.366993

Au	3.362124	0.000000	2.366993
Au	3.362124	2.911685	2.366993
Au	0.000000	0.000000	0.000000
Au	2.521593	1.455842	0.000000
Au	5.043187	2.911685	0.000000

XYZ format coordinates for Geo. 2:

52

BDA/Au111 Geo. 2

C	4.761413451	4.019274501	10.522261754
C	2.620895606	3.443966919	12.262450780
C	3.946629270	3.451639331	12.723128482
C	3.451380398	3.970882823	10.059268094
C	5.001791441	3.737030845	11.864924817
C	2.393848463	3.694654121	10.902427675
H	4.148516089	3.250588215	13.771324166
H	3.257517136	4.149955505	9.004022563
H	6.017168085	3.762421231	12.252915793
H	1.388867942	3.658540452	10.489816377
H	6.733942585	4.147050554	9.981433813
H	0.692925395	2.941910612	12.718771470
H	5.803247145	5.361520897	9.365644656
H	1.772841755	2.788861356	14.005180670
N	5.812986221	4.366152204	9.611924720
N	1.561194696	3.246078170	13.131982881
Au	0.964117351	-0.348343041	7.742372139
Au	4.530236087	1.030773970	7.687033493

Au	7.141760993	0.161546092	7.333429351
Au	2.061175236	2.157113304	7.524095839
Au	5.767629850	3.550809856	7.398783007
Au	8.365987446	2.611175034	7.352368745
Au	3.766769803	5.469249307	7.103858434
Au	7.871989956	6.345623619	7.378606960
Au	10.100949264	4.767738419	7.051396140
Au	0.628253963	1.975131362	4.857349387
Au	4.359172220	1.190983249	5.010798781
Au	6.740363878	2.519484037	4.977290905
Au	2.860036358	3.546187156	5.119587743
Au	5.298448399	4.889206840	4.896292938
Au	8.182069279	4.993620986	4.899221627
Au	3.838905079	7.338305521	4.851147983
Au	6.682169373	7.428123119	4.979732177
Au	10.318582343	6.681125101	5.036800014
Au	1.507965000	0.870624000	2.462496000
Au	4.523894000	0.870624000	2.462496000
Au	7.539824000	0.870624000	2.462496000
Au	3.015929000	3.482495000	2.462496000
Au	6.031859000	3.482495000	2.462496000
Au	9.047789000	3.482495000	2.462496000
Au	4.523894000	6.094367000	2.462496000
Au	7.539824000	6.094367000	2.462496000
Au	10.555753000	6.094367000	2.462496000
Au	0.000000000	0.000000000	0.000000000
Au	3.015929000	0.000000000	0.000000000
Au	6.031859000	0.000000000	0.000000000

Au	1.507965000	2.611871000	0.000000000
Au	4.523894000	2.611871000	0.000000000
Au	7.539824000	2.611871000	0.000000000
Au	3.015929000	5.223743000	0.000000000
Au	6.031859000	5.223743000	0.000000000
Au	9.047789000	5.223743000	0.000000000

XYZ format coordinates for Geo. 3:

52
BDA/Au111 Geo. 3

C	2.730355	2.522484	10.070164
C	5.422029	2.522759	10.925045
C	4.735766	3.730650	10.704206
C	3.410923	1.314465	10.276190
C	3.409572	3.730663	10.279437
C	4.737030	1.314724	10.700964
H	5.252808	4.683311	10.855477
H	2.903116	0.363397	10.082341
H	2.900752	4.681685	10.088120
H	5.255090	0.362164	10.849473
H	0.874735	3.363748	9.711786
H	7.264235	1.673163	11.253534
H	0.875384	1.680238	9.712041
H	7.263835	3.372660	11.255507
N	1.420943	2.522159	9.519558
N	6.728310	2.522613	11.407515
Au	-0.011328	-0.021809	7.093648
Au	1.432353	2.519782	7.071760
Au	2.916514	5.057871	7.063904
Au	2.914489	-0.022022	7.066985
Au	4.382766	2.519448	7.050173
Au	5.824010	5.041463	7.104085
Au	5.822985	-0.003273	7.101907
Au	7.253042	2.521951	7.093094
Au	8.720242	5.058489	7.096251
Au	-1.460520	-0.835989	4.700900
Au	-0.003236	1.679730	4.724558
Au	1.449835	4.198133	4.724686

Au	1. 450752	-0. 844558	4. 710308
Au	2. 901150	1. 682475	4. 725055
Au	4. 369957	4. 207025	4. 706791
Au	4. 371940	-0. 840565	4. 703816
Au	5. 826000	1. 672797	4. 702075
Au	7. 277906	4. 202270	4. 714493
Au	10. 190898	5. 883718	2. 366993
Au	7. 279213	0. 840531	2. 366993
Au	8. 735055	3. 362125	2. 366993
Au	4. 367527	5. 883718	2. 366993
Au	1. 455842	0. 840531	2. 366993
Au	2. 911685	3. 362125	2. 366993
Au	7. 279212	5. 883718	2. 366993
Au	4. 367527	0. 840531	2. 366993
Au	5. 823370	3. 362125	2. 366993
Au	0. 000000	0. 000000	0. 000000
Au	1. 455843	2. 521594	0. 000000
Au	2. 911685	5. 043188	0. 000000
Au	2. 911685	0. 000000	0. 000000
Au	4. 367527	2. 521594	0. 000000
Au	5. 823370	5. 043188	0. 000000
Au	5. 823370	0. 000000	0. 000000
Au	7. 279213	2. 521594	0. 000000
Au	8. 735055	5. 043188	0. 000000

XYZ format coordinates for Geo. 4:

53

BDA/Au111 Geo. 4

C	1. 891566814	4. 576038109	11. 573503922
C	1. 832116814	4. 543150409	14. 408967922
C	2. 442723814	3. 513916254	13. 685161622
C	1. 274174814	5. 601394909	12. 297214522
C	2. 470823814	3. 528774977	12. 297576922
C	1. 245677014	5. 585894609	13. 684983222
H	2. 905559814	2. 687522649	14. 219049422
H	0. 803113014	6. 424243409	11. 765379422
H	2. 947296814	2. 707463029	11. 768434522
H	0. 763359114	6. 403440209	14. 215219522
H	2. 598312814	4. 012539629	9. 744261222
H	1. 123661014	5. 089952909	16. 242661122
H	1. 782871814	5. 467323309	9. 739604922

H	1. 956700814	3. 648590329	16. 235336122
N	1. 866445814	4. 560087409	10. 173820022
N	1. 866410814	4. 560116309	15. 809484122
Au	0. 000000604	3. 482494306	9. 268659967
Au	0. 000000000	0. 000000000	7. 201817163
Au	-1. 507964117	2. 611870469	7. 201817163
Au	-3. 015928234	5. 223740938	7. 201817163
Au	3. 015928239	0. 000000000	7. 201817163
Au	1. 507964122	2. 611870469	7. 201817163
Au	0. 000000005	5. 223740938	7. 201817163
Au	6. 031856478	0. 000000000	7. 201817163
Au	4. 523892361	2. 611870469	7. 201817163
Au	3. 015928244	5. 223740938	7. 201817163
Au	0. 000000000	1. 741247675	4. 842043812
Au	-1. 507964117	4. 353118144	4. 842043812
Au	-3. 015928234	6. 964988613	4. 842043812
Au	3. 015928239	1. 741247675	4. 842043812
Au	1. 507964122	4. 353118144	4. 842043812
Au	0. 000000005	6. 964988613	4. 842043812
Au	6. 031856478	1. 741247675	4. 842043812
Au	4. 523892361	4. 353118144	4. 842043812
Au	3. 015928244	6. 964988613	4. 842043812
Au	1. 507964721	0. 870623837	2. 462496078
Au	0. 000000604	3. 482494306	2. 462496078
Au	-1. 507963513	6. 094364775	2. 462496078
Au	4. 523892960	0. 870623837	2. 462496078
Au	3. 015928843	3. 482494306	2. 462496078
Au	1. 507964726	6. 094364775	2. 462496078
Au	7. 539821199	0. 870623837	2. 462496078
Au	6. 031857082	3. 482494306	2. 462496078
Au	4. 523892965	6. 094364775	2. 462496078
Au	0. 000000000	0. 000000000	0. 000000000
Au	-1. 507964117	2. 611870469	0. 000000000
Au	-3. 015928234	5. 223740938	0. 000000000
Au	3. 015928239	0. 000000000	0. 000000000
Au	1. 507964122	2. 611870469	0. 000000000
Au	0. 000000005	5. 223740938	0. 000000000
Au	6. 031856478	0. 000000000	0. 000000000
Au	4. 523892361	2. 611870469	0. 000000000
Au	3. 015928244	5. 223740938	0. 000000000

13) DFT and GW bandstructure for the BDA layer as in Geo. 4

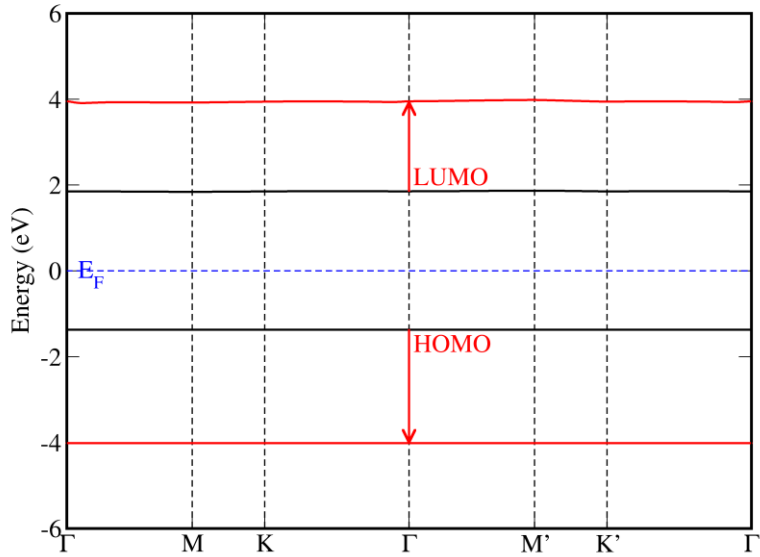


Figure S5. DFT (Black) and GW (Red) bandstructure for BDA molecular layer as in Geo. 4, along the k-path $\Gamma \rightarrow M \rightarrow K \rightarrow \Gamma \rightarrow M' \rightarrow K' \rightarrow \Gamma$ calculated with 4×4 k-mesh sampling, and 12 Ry epsilon cutoff in GW calculation. Bandwidth for HOMO and LUMO bands are 0.00055 eV (0.00066 eV) and 0.025 eV (0.073 eV) respectively, for the DFT (GW) results. They are not dispersive across the Brillouin zone. GW HOMO-LUMO gap at Γ for the layer is 7.959 eV, while the corresponding Wigner-Seitz truncation gives 8.169 eV. So the intra-molecular layer polarization effect is only 0.21 eV.

14) GW projected molecular level dispersion across the Brillouin zone

We also performed slab truncation GW projection calculations of the HOMO and LUMO levels of BDA as in Geo. 4 at another three k-points in the Brillouin zone (BZ). The results are summarized in the table below (with respect to the Fermi level). There is seen to be little dispersion even for the projected levels from the molecule-metal hybrid slab. This indicates the molecular band gap renormalization we observe is not from BZ dispersion of the adsorbed molecular layer. A molecular layer GW projected bandstructure is currently beyond the reach of our computational capabilities.

Table S9 Slab GW HOMO and LUMO levels for Geometry 4

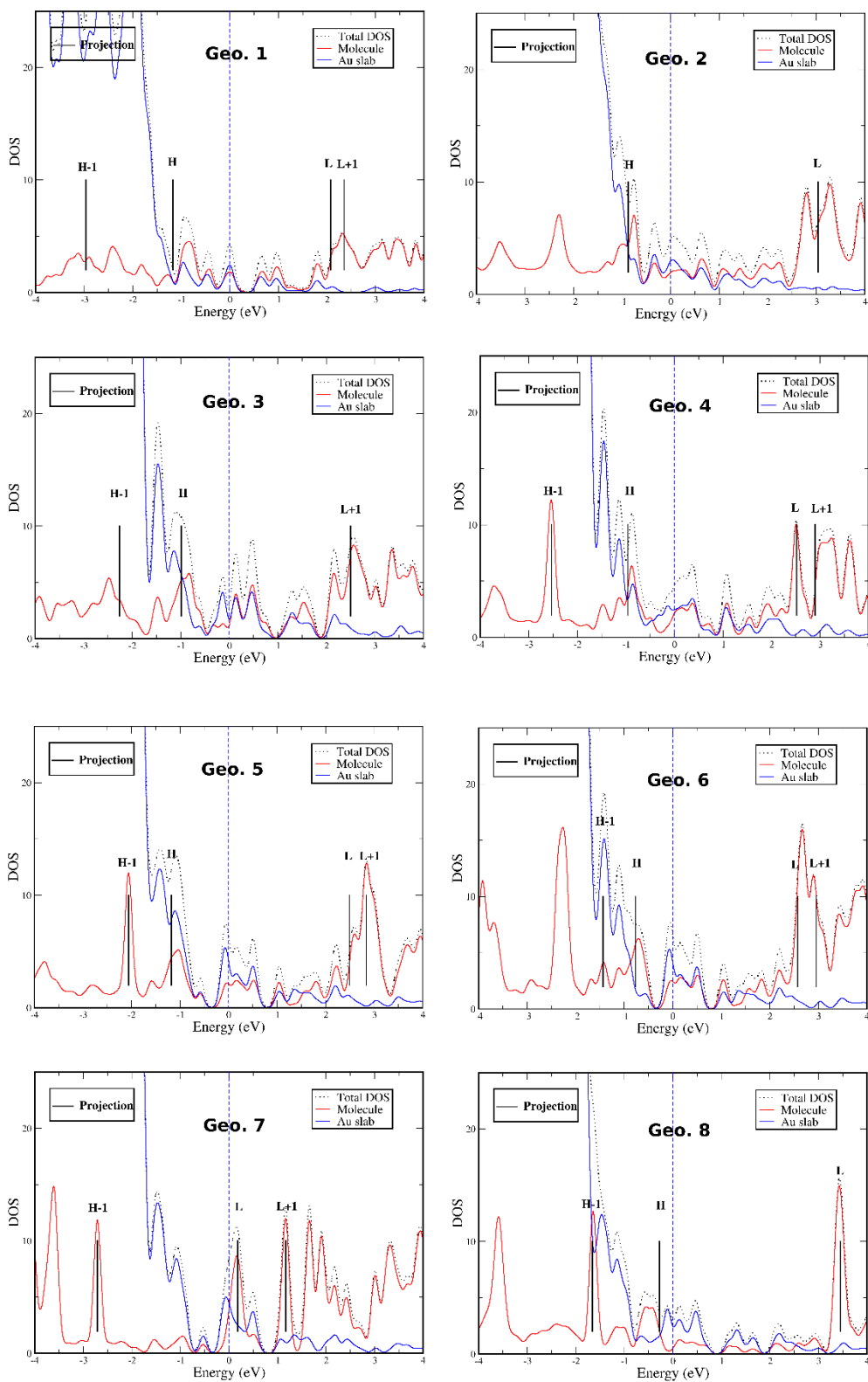
(eV)	Γ	$K=(0.0, 0.5, 0.0)$	$K=(0.5, 0.0, 0.0)$	$K=(0.5, 0.5, 0.0)$
HOMO	-1.344	-1.345	-1.345	-1.346
LUMO	+4.230	+4.208	+4.207	+4.251

15) Calculated image charge correction energy for the hybridized slabs

Table S10: Image charge model correction energy for various MO levels in the hybridized geometries investigated in this work. Here, we compare the image charge correction we have computed with that assuming a unit of point charge (point charge method) at the ring center or in the middle of the molecule (Geometries 6 and 7 where there are two rings). The image plane is taken to be 0.9 Å above the Au(111) surface.

	Geo. 1 HOMO	Geo. 2 HOMO	Geo. 3 HOMO	Geo. 4 HOMO	Geo. 5 HOMO	Geo. 6 HOMO
Image charge correction used in the main text (eV)	0.9612	1.2181	1.3059	0.8174	0.8129	0.5913
Distance of point charge from image plane (Å)	4.126	3.094	2.515	4.889	4.892	7.043
Point charge method (eV)	0.8725	1.1630	1.4314	0.7363	0.7358	0.5112
	Geo. 7 LUMO	Geo. 8 HOMO	Geo. 9 HOMO	Geo. 10 HOMO	Geo. 11 HOMO	
Image charge correction used in the main text (eV)	0.5631	0.8639	0.7729	0.5937	2.3382	
Distance of point charge from image plane (Å)	6.864	5.447	6.590	6.576	3.957	
Point charge method (eV)	0.5239	0.6609	0.5463	0.5474	0.9097	

16) Projected density of states together with our DFT starting points marked for Geo.'s 1-11 investigated in this work.



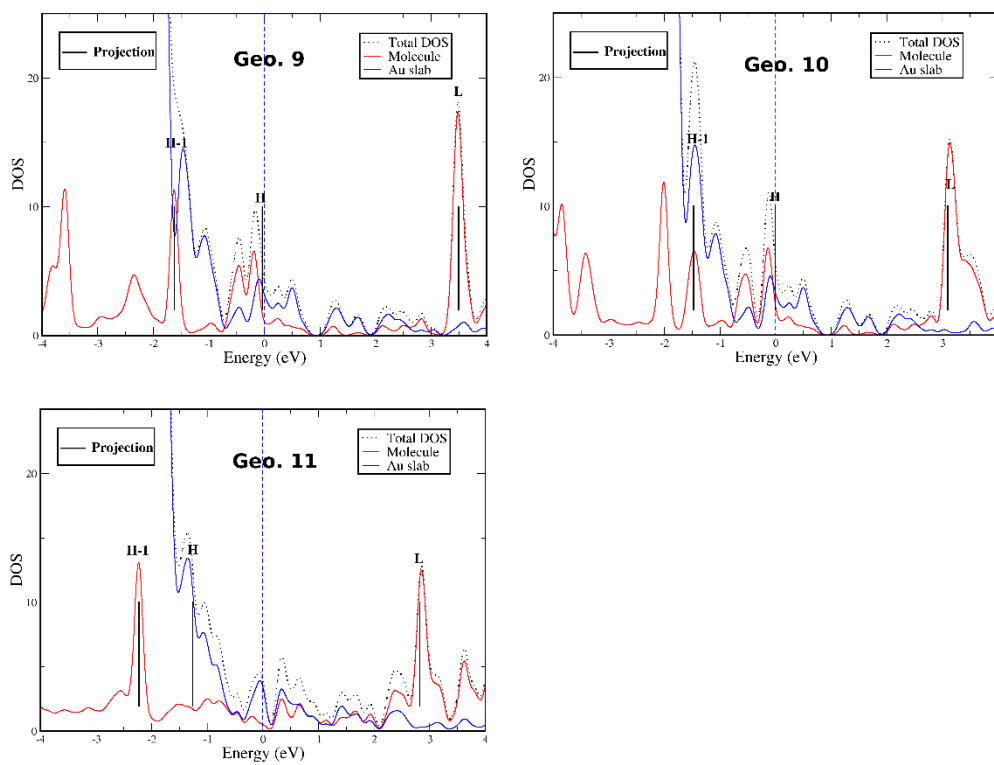


Figure S6. Projected density of states plots, with our wavefunction based projected DFT HOMO-1 (**H-1**), HOMO (**H**), LUMO (**L**), and LUMO+1 (**L+1**) starting point levels marked on the same plot.

17) Table S11 is given in the next page.

Spectroscopically undefined levels (without a well-defined peak) are omitted.

Table S11: Energy levels for various structures. Fermi levels are absolute values for each calculation, while all the rest data are given with respective to the molecule/metal slab Fermi level of each case.									
System	DFT HOMO	GW HOMO (Slab)	GW HOMO (Box)	ImageMeth HOMO	DFT LUMO	GW LUMO (Slab)	GW LUMO (Box)	ImageMeth LUMO	E_Fermi
4 BDA-Ti/3x3Au111 NoAd PBE-D2 (2)	-0.873	-1.3332	-3.181	-2.5698	3.0364	3.7004	3.5394	3.8748	3.8352
5 BDA-Ti/3x3Au111 W/Ad PBE-D2	-0.2852	-0.7426	-2.6012	-2.221	2.9602	3.35	3.2152	4.0993	4.0491
6 BDA-Ti/Sqr(3)^2R30 Au NoAd VdW (1)	-1.1726	-1.6428	-4.2112	-3.1254	2.0744	2.7894	None	3.2501	5.2874
7 BDA-Ti/Sqr(3)^2R30 Au/W/Ad VdW	-2.5634	-3.4123	-5.5623	-4.8104	0.619	Wg Occ.	None	2.0305	6.6385
8 BDA-Face/3x3Au111 NoAd VdW (3)	-0.99	-1.2988	None	-2.5981	N.A.	N.A.	None	None	5.9661
9 BDA-Face/3x3Au111 W/Ad QE	-1.653	-2.2559	None	-3.8025	1.8643	2.6849	None	3.1377	4.3414
10 BDA-Face/3x3Au111 NoAd QE	-0.8712	-1.1779	None	-2.5155	N.A.	N.A.	None	None	4.7646
11 BDA-Vert/3x3Au111 W/Ad QE (4)	-0.9582	-1.3443	-3.1074	-3.0548	2.5157	4.2303	4.236	3.8222	3.6168
12 Ibid (Stat.-COHSEX)	-0.9582	-2.5428	-4.7966	as above	2.5157	3.3967	3.2504	as above	ibid
13 BDA-Vert/3x3Au111 W/Ad VdW	-1.059	-1.4883	-3.3575	n.a.	2.8243	2.8919	2.5205	n.a.	4.2737
14 BDA-LinChain/Au111 NoAd @G_Li	-0.571	-0.7501	None	N.A.	2.9374	4.2039	None	N.A.	4.2096
15 FABDDA-Vert/3x3Au111 w/Ad VdW (5)	-1.1804	-1.7128	-3.5074	-3.3345	2.4934	3.5688	3.3388	3.662	4.3361
16 BPDDA-Vert/3x3Au111 w/Ad VdW (6)	-0.7649	-1.1672	-2.9356	-2.7026	2.5765	3.6686	3.338	3.6684	3.522
17 Bpyd-Vert/3x3Au111 w/Ad VdW (7)	N.A.	N.A.	N.A.	0.1782	0.3992	1.6856	1.5081	4.0253	4.0253
18 Ibid (Stat.-COHSEX)	N.A.	N.A.	as above	0.1782	Wg Occ.	0.5158	as above	ibid	ibid
19 BDA-Vert/4x4Au1114L W/Ad VdW (4")	-0.5856	N.A.	-2.3749	-2.6822	2.8016	N.A.	4.2129	4.1081	3.0178
20 BDA-Vert/3x3Au1116L W/Ad VdW (4)	-0.8052	N.A.	-2.7759	-2.9018	2.6282	N.A.	4.2318	3.9347	5.4439
21 BDA-Vert/Sqr(3)^2R30W/ Ad VdW	-1.1381	-1.7833	-4.4266	-3.2338	1.5964	Wg Occ.	Wg Occ.	2.9032	6.0106
22 Au/BDA-Vt/Au Sqr(3)^2R30 Ad Junc	-1.2142	-1.484	-4.0579	-2.9532	1.2977	Wg Occ.	Wg Occ.	2.2947	9.6787
23 Au/BDA-Vt/Au 3x3 Ad Junc	-0.5855	None	-2.146	-2.3212	2.6448	None	4.0031	3.641	6.5264
24 Au/BP-Vt/Au 3x3 Ad Junc	N.A.	N.A.	N.A.	0.3879	None	0.8386	1.4885	6.5612	4.2709
25 BDA/Sqr(3)^2R30 NoAd PBE-D2 (1')	-1.087	-1.6984	None	-3	2.3667	2.9918	None	3.4684	4.2709
26 BT/Sqr(3)^2R30 W/Ad PBE-D2	-0.3716	-1.0261	None	-2.2327	2.6472	3.6602	None	3.956	4.5505
27 BT-Ti/3x3Au1114L w/Ad VdW (8)	-0.273	-0.7212	-2.2252	-2.5551	3.4541	4.8332	4.8044	4.8734	3.4517
28 Ibid (Stat.-COHSEX)	-0.273	-1.7232	-3.6594	as above	3.4541	3.8739	3.7652	as above	ibid
29 BT-Rx/3x3Au1114L NoAd VdW (11)	-1.2639	-1.8048	-3.5968	-2.0717	2.8252	4.4558	4.4492	3.9909	3.6974
30 Ibid (Stat.-COHSEX)	-1.2639	-2.9642	-5.2787	as above	2.8252	3.4946	3.4063	as above	ibid
31 BT-Rx/3x3Au1114L Ad VdW (9)	-0.0362	-0.2711	-2.4786	-2.4093	3.4958	4.8948	5.2038	5.0271	3.4169
32 Ibid (Stat.-COHSEX)	-0.0362	-1.2705	-4.096	as above	3.4958	3.8763	4.1818	as above	ibid
33 BT-Rx/3x3Au1114L Ad VdW	-0.1586	None	-2.15	-2.5317	3.4257	None	4.9231	4.957	5.2395
34 BDT-Vert/3x3Au1114L W/Ad VdW (10)	-0.0044	-0.3444	-2.5532	-2.0557	3.1	4.3967	4.741	4.8325	3.6124
35 BDT-Vert/3x3Au1114L W/Ad VdW	-0.1127	None	-2.2746	-2.164	None	4.4643	4.7652	3.0327	5.4144

References

- [1] G. Kresse and J. Furthmuller, Computational Materials Science **6**, 15 (1996).
- [2] P. Giannozzi *et al.*, Journal of Physics-Condensed Matter **21**, 19, 395502 (2009).
- [3] S. Grimme, Journal of Computational Chemistry **27**, 1787 (2006).
- [4] M. Dion, H. Rydberg, E. Schroder, D. C. Langreth, and B. I. Lundqvist, Physical Review Letters **92**, 4, 246401 (2004).
- [5] J. Klimes, D. R. Bowler, and A. Michaelides, Physical Review B **83**, 195131 (2011).
- [6] M. Dell'Angela *et al.*, Nano Letters **10**, 2470 (2010).
- [7] G. Li, T. Rangel, Z.-F. Liu, V. R. Cooper, and J. B. Neaton, Physical Review B **93**, 125429 (2016).
- [8] G. Henkelman, A. Arnaldsson, and H. Jonsson, Computational Materials Science **36**, 354 (2006).
- [9] J. Deslippe, G. Samsonidze, D. A. Strubbe, M. Jain, M. L. Cohen, and S. G. Louie, Computer Physics Communications **183**, 1269 (2012).
- [10] T. Rangel, D. Kecik, P. E. Trevisanutto, G. M. Rignanese, H. Van Swygenhoven, and V. Olevano, Physical Review B **86**, 125125 (2012).
- [11] J. Deslippe, G. Samsonidze, M. Jain, M. L. Cohen, and S. G. Louie, Physical Review B **87**, 165124 (2013).
- [12] Y. J. Zheng *et al.*, Acs Nano **10**, 2476 (2016).
- [13] D. A. Egger, Z. F. Liu, J. B. Neaton, and L. Kronik, Nano Letters **15**, 2448 (2015).
- [14] J. M. Soler, E. Artacho, J. D. Gale, A. Garcia, J. Junquera, P. Ordejon, and D. Sanchez-Portal, Journal of Physics-Condensed Matter **14**, 2745, Pii s0953-8984(02)30737-9 (2002).
- [15] A. Kokalj, Computational Materials Science **28**, 155 (2003).
- [16] S. Sharifzadeh, I. Tamblyn, P. Doak, P. T. Darancet, and J. B. Neaton, European Physical Journal B **85**, 323 (2012).
- [17] T. K. Haxton, H. Zhou, I. Tamblyn, D. Eom, Z. H. Hu, J. B. Neaton, T. F. Heinz, and S. Whitelam, Physical Review Letters **111**, 5, 265701 (2013).

XYZ format coordinates for Geo. 5:

=====

53

FBDA/Au111 Geo. 5

C	3. 346936459	1. 933185327	11. 504639189
C	3. 284275559	1. 898938327	14. 371124289
C	3. 891758959	0. 882371327	13. 631277989
C	2. 740061959	2. 950213427	12. 244251689
C	3. 922006159	0. 899107327	12. 245656989
C	2. 709002959	2. 933199927	13. 630192789

F	4.466391559	-0.144357673	14.304729489
F	2.174253959	3.981608427	11.570697789
F	4.529808959	-0.109429673	11.573615989
F	2.107283159	3.945006327	14.302213689
H	4.046689959	1.358908327	9.690505489
H	2.583575959	2.465780227	16.188327589
H	3.217785559	2.825453727	9.687817089
H	3.428218359	1.008035327	16.187054589
N	3.322287359	1.918124327	10.117536089
N	3.310993659	1.914196327	15.758096589
Au	1.455842	0.840531	9.212376
Au	0.000000	0.000000	7.145576
Au	1.455842	2.521594	7.145576
Au	2.911685	5.043187	7.145576
Au	2.911685	0.000000	7.145576
Au	4.367527	2.521594	7.145576
Au	5.823370	5.043187	7.145576
Au	5.823370	0.000000	7.145576
Au	7.279213	2.521594	7.145576
Au	8.735055	5.043187	7.145576
Au	-1.455842	-0.840530	4.740462
Au	0.000000	1.681062	4.740462
Au	1.455842	4.202656	4.740462
Au	1.455842	-0.840530	4.740462
Au	2.911685	1.681062	4.740462
Au	4.367527	4.202656	4.740462
Au	4.367527	-0.840530	4.740462
Au	5.823370	1.681062	4.740462
Au	7.279212	4.202656	4.740462
Au	-2.911684	-1.681061	2.366993
Au	-1.455842	0.840531	2.366993
Au	0.000000	3.362125	2.366993
Au	0.000000	-1.681061	2.366993
Au	1.455842	0.840531	2.366993
Au	2.911685	3.362125	2.366993
Au	2.911685	-1.681061	2.366993
Au	4.367527	0.840531	2.366993
Au	5.823370	3.362125	2.366993
Au	0.000000	0.000000	0.000000
Au	1.455842	2.521594	0.000000
Au	2.911685	5.043187	0.000000
Au	2.911685	0.000000	0.000000
Au	4.367527	2.521594	0.000000
Au	5.823370	5.043187	0.000000
Au	5.823370	0.000000	0.000000

Au	7.279213	2.521594	0.000000
Au	8.735055	5.043187	0.000000

XYZ format coordinates for Geo. 6:

63

BPDA/Au111 Geo. 6

C	3.355147993	1.929198734	11.507437954
C	3.335166093	1.898626734	15.824901554
C	2.746321293	2.959346734	12.235939054
C	2.251890783	2.406469734	16.555333154
C	2.744683193	2.943040834	13.621835254
C	2.236940743	2.406404734	17.941023154
C	3.340460893	1.904830734	14.351695054
C	3.315899293	1.887271734	18.669003154
C	3.937884493	0.875307734	13.611186954
C	4.408231393	1.382604734	17.951214154
C	3.946577693	0.880544734	12.224902154
C	4.411557793	1.389212734	16.565165554
H	2.279821273	3.786867134	11.705902554
H	1.383887413	2.786858534	16.024913754
H	2.291950583	3.775274234	14.152350454
H	1.373523833	2.802698134	18.470975154
H	4.387785293	0.035310734	14.132204554
H	5.269483193	0.994900734	18.490933154
H	4.405103293	0.055064734	11.685146354
H	5.285158793	1.009420734	16.043815654
H	4.025957493	1.359131734	9.659574754
H	3.180130793	2.809911734	9.668415554
H	2.427767873	1.997757734	20.508727154
H	3.940838193	1.269188734	20.517403154
N	3.322287393	1.918023734	10.117536054
N	3.327639693	1.925412734	20.058623154
Au	1.455842	0.840531	9.212376
Au	0.000000	0.000000	7.145576
Au	1.455842	2.521594	7.145576
Au	2.911685	5.043187	7.145576
Au	2.911685	0.000000	7.145576
Au	4.367527	2.521594	7.145576
Au	5.823370	5.043187	7.145576
Au	5.823370	0.000000	7.145576
Au	7.279213	2.521594	7.145576
Au	8.735055	5.043187	7.145576
Au	-1.455842	-0.840530	4.740462

Au	0. 000000	1. 681062	4. 740462
Au	1. 455842	4. 202656	4. 740462
Au	1. 455842	-0. 840530	4. 740462
Au	2. 911685	1. 681062	4. 740462
Au	4. 367527	4. 202656	4. 740462
Au	4. 367527	-0. 840530	4. 740462
Au	5. 823370	1. 681062	4. 740462
Au	7. 279212	4. 202656	4. 740462
Au	-2. 911684	-1. 681061	2. 366993
Au	-1. 455842	0. 840531	2. 366993
Au	0. 000000	3. 362125	2. 366993
Au	0. 000000	-1. 681061	2. 366993
Au	1. 455842	0. 840531	2. 366993
Au	2. 911685	3. 362125	2. 366993
Au	2. 911685	-1. 681061	2. 366993
Au	4. 367527	0. 840531	2. 366993
Au	5. 823370	3. 362125	2. 366993
Au	0. 000000	0. 000000	0. 000000
Au	1. 455842	2. 521594	0. 000000
Au	2. 911685	5. 043187	0. 000000
Au	2. 911685	0. 000000	0. 000000
Au	4. 367527	2. 521594	0. 000000
Au	5. 823370	5. 043187	0. 000000
Au	5. 823370	0. 000000	0. 000000
Au	7. 279213	2. 521594	0. 000000
Au	8. 735055	5. 043187	0. 000000

XYZ format coordinates for Geo. 7:

57

BP/Au111 Geo. 7

C	2. 609926793	0. 821302516	12. 056242343
C	0. 448298316	0. 339810507	17. 767854339
C	2. 649631142	0. 833870231	13. 435745220
C	0. 393356000	0. 323579453	16. 379715619
C	1. 460313362	0. 842881731	14. 176526920
C	1. 464719776	0. 842743837	15. 643683747
C	0. 266784301	0. 848458909	13. 442073723
C	2. 540800797	1. 358348077	16. 375483503
C	0. 298820733	0. 845534869	12. 062005361
C	2. 492748462	1. 338967827	17. 763943210
H	3. 516483889	0. 798050830	11. 459771484
H	-0. 371864948	-0. 076305610	18. 349660787

H	3.611368932	0.810875717	13.934398978
H	-0.462652251	-0.117662284	15.879364189
H	-0.691999414	0.878410069	13.946053359
H	3.395731724	1.798424833	15.872675457
H	-0.611111453	0.864182907	11.470558529
H	3.315778389	1.752749059	18.343104391
N	1.452606489	0.827735032	11.365970727
N	1.471978177	0.839046221	18.467563258
Au	1.455842000	0.840531000	9.212376000
Au	0.000000000	0.000000000	7.145576000
Au	1.455842000	2.521594000	7.145576000
Au	2.911685000	5.043187000	7.145576000
Au	2.911685000	0.000000000	7.145576000
Au	4.367527000	2.521594000	7.145576000
Au	5.823370000	5.043187000	7.145576000
Au	5.823370000	0.000000000	7.145576000
Au	7.279213000	2.521594000	7.145576000
Au	8.735055000	5.043187000	7.145576000
Au	-1.455842000	-0.840530000	4.740462000
Au	-0.000000000	1.681062000	4.740462000
Au	1.455842000	4.202656000	4.740462000
Au	1.455842000	-0.840530000	4.740462000
Au	2.911685000	1.681062000	4.740462000
Au	4.367527000	4.202656000	4.740462000
Au	4.367527000	-0.840530000	4.740462000
Au	5.823370000	1.681062000	4.740462000
Au	7.279212000	4.202656000	4.740462000
Au	-2.911684000	-1.681061000	2.366993000
Au	-1.455842000	0.840531000	2.366993000
Au	-0.000000000	3.362125000	2.366993000
Au	-0.000000000	-1.681061000	2.366993000
Au	1.455842000	0.840531000	2.366993000
Au	2.911685000	3.362125000	2.366993000
Au	2.911685000	-1.681061000	2.366993000
Au	4.367527000	0.840531000	2.366993000
Au	5.823370000	3.362125000	2.366993000
Au	0.000000000	0.000000000	0.000000000
Au	1.455842000	2.521594000	0.000000000
Au	2.911685000	5.043187000	0.000000000
Au	2.911685000	0.000000000	0.000000000
Au	4.367527000	2.521594000	0.000000000
Au	5.823370000	5.043187000	0.000000000
Au	5.823370000	0.000000000	0.000000000
Au	7.279213000	2.521594000	0.000000000
Au	8.735055000	5.043187000	0.000000000

XYZ format coordinates for Geo. 8:

49

BT/Au111 Geo. 8

C	2. 150145	-1. 230141	14. 477068
C	3. 115240	-0. 239798	14. 271947
C	1. 018261	-1. 278469	13. 655580
C	1. 811997	0. 660244	12. 432239
C	0. 843390	-0. 339825	12. 640182
C	2. 953773	0. 698985	13. 253397
H	2. 279572	-1. 963974	15. 275338
H	4. 003986	-0. 199515	14. 906179
H	0. 260375	-2. 050132	13. 811606
H	-0. 046466	-0. 365081	12. 006510
H	3. 709088	1. 469532	13. 082018
S	1. 587966	1. 944259	11. 238962
Au	1. 465806	0. 896358	9. 218989
Au	-0. 039413	-0. 033752	7. 150378
Au	1. 458566	2. 592555	7. 053531
Au	2. 911708	5. 051297	7. 108723
Au	2. 941963	-0. 020757	7. 118739
Au	4. 381521	2. 531892	7. 098454
Au	5. 824805	5. 037709	7. 118122
Au	5. 822330	0. 004812	7. 106397
Au	7. 270741	2. 529382	7. 098300
Au	8. 731442	5. 053135	7. 117217
Au	-1. 441147	-0. 828900	4. 739646
Au	-0. 001690	1. 669536	4. 742193
Au	1. 451877	4. 211063	4. 714260
Au	1. 449829	-0. 831777	4. 749635
Au	2. 916351	1. 681528	4. 720239
Au	4. 367039	4. 207519	4. 722154
Au	4. 357423	-0. 834021	4. 729552
Au	5. 823437	1. 678444	4. 717889
Au	7. 281885	4. 209522	4. 722643
Au	-2. 911684	-1. 681061	2. 366993
Au	-1. 455842	0. 840531	2. 366993
Au	0. 000000	3. 362125	2. 366993
Au	0. 000000	-1. 681061	2. 366993
Au	1. 455842	0. 840531	2. 366993
Au	2. 911685	3. 362125	2. 366993
Au	2. 911685	-1. 681061	2. 366993

Au	4. 367527	0. 840531	2. 366993
Au	5. 823370	3. 362125	2. 366993
Au	0. 000000	0. 000000	0. 000000
Au	1. 455843	2. 521594	0. 000000
Au	2. 911685	5. 043187	0. 000000
Au	2. 911685	0. 000000	0. 000000
Au	4. 367527	2. 521594	0. 000000
Au	5. 823370	5. 043187	0. 000000
Au	5. 823370	0. 000000	0. 000000
Au	7. 279213	2. 521594	0. 000000
Au	8. 731442	5. 053135	0. 000000

XYZ format coordinates for Geo. 9:

49

BT/Au111 Geo. 9

C	1. 426690	0. 839128	15. 979084
C	1. 437812	0. 838811	13. 179546
C	0. 219173	0. 838967	15. 272281
C	0. 214734	0. 838797	13. 879280
C	2. 639688	0. 838943	15. 281778
C	2. 655425	0. 838801	13. 888760
H	-0. 730831	0. 838986	15. 812101
H	-0. 722712	0. 839139	13. 320462
H	3. 585295	0. 838949	15. 829356
H	3. 597467	0. 839153	13. 337756
H	1. 422346	0. 839351	17. 071012
S	1. 442356	0. 838610	11. 425965
Au	1. 450868	0. 841494	9. 156417
Au	-0. 052733	-0. 034792	7. 091561
Au	1. 453200	2. 582392	7. 096040
Au	2. 907229	5. 041691	7. 093721
Au	2. 958261	-0. 034232	7. 093453
Au	4. 375841	2. 526106	7. 080925
Au	5. 820825	5. 029961	7. 083813
Au	5. 820347	-0. 002465	7. 089806
Au	7. 265927	2. 526024	7. 081017
Au	8. 734023	5. 042040	7. 093887
Au	2. 920018	6. 727657	4. 719918
Au	0. 002202	1. 677897	4. 721198
Au	1. 454337	4. 189516	4. 719575
Au	5. 821989	6. 724917	4. 718755
Au	2. 906571	1. 677815	4. 721424

Au	4. 361479	4. 203880	4. 712465
Au	8. 723205	6. 727948	4. 720487
Au	5. 821971	1. 673987	4. 711652
Au	7. 282404	4. 203845	4. 712494
Au	10. 190896	5. 883717	2. 366993
Au	7. 279211	0. 840531	2. 366993
Au	8. 735053	3. 362125	2. 366993
Au	4. 367527	5. 883717	2. 366993
Au	1. 455842	0. 840531	2. 366993
Au	2. 911685	3. 362125	2. 366993
Au	7. 279212	5. 883717	2. 366993
Au	4. 367527	0. 840531	2. 366993
Au	5. 823370	3. 362125	2. 366993
Au	0. 000000	0. 000000	0. 000000
Au	1. 455843	2. 521594	0. 000000
Au	2. 911685	5. 043187	0. 000000
Au	2. 911685	0. 000000	0. 000000
Au	4. 367527	2. 521594	0. 000000
Au	5. 823370	5. 043187	0. 000000
Au	5. 823370	0. 000000	0. 000000
Au	7. 279213	2. 521594	0. 000000
Au	8. 735055	5. 043187	0. 000000

XYZ format coordinates for Geo. 10:

50
BDA/Au111 Geo. 10

C	1. 450287	0. 839070	15. 967575
C	1. 436239	0. 839678	13. 152452
C	0. 232534	0. 839533	15. 261061
C	0. 222492	0. 839878	13. 872808
C	2. 660110	0. 839449	15. 250630
C	2. 655280	0. 839722	13. 862775
H	-0. 714431	0. 839709	15. 807552
H	-0. 722960	0. 840254	13. 327235
H	3. 613864	0. 839714	15. 784193
H	3. 595005	0. 840010	13. 307438
H	2. 714658	0. 835950	17. 932905
S	1. 380408	0. 838385	17. 723131
S	1. 441391	0. 837451	11. 411168
Au	1. 441553	0. 837765	9. 135625
Au	-0. 057260	-0. 039232	7. 074550
Au	1. 453108	2. 584203	7. 083807
Au	2. 906261	5. 039850	7. 092668

Au	2. 958892	-0. 036463	7. 080940
Au	4. 376632	2. 525972	7. 079947
Au	5. 820942	5. 029329	7. 083890
Au	5. 818905	-0. 002927	7. 088006
Au	7. 265678	2. 525811	7. 080161
Au	8. 734281	5. 041441	7. 093029
Au	2. 917288	6. 725523	4. 715117
Au	0. 001077	1. 678335	4. 716452
Au	1. 454314	4. 190536	4. 715515
Au	5. 822172	6. 722654	4. 713393
Au	2. 907832	1. 678137	4. 717274
Au	4. 362059	4. 203358	4. 712223
Au	8. 724665	6. 726484	4. 716837
Au	5. 822145	1. 674022	4. 711135
Au	7. 282074	4. 203297	4. 712359
Au	10. 190896	5. 883717	2. 366993
Au	7. 279211	0. 840531	2. 366993
Au	8. 735053	3. 362125	2. 366993
Au	4. 367527	5. 883717	2. 366993
Au	1. 455842	0. 840531	2. 366993
Au	2. 911685	3. 362125	2. 366993
Au	7. 279212	5. 883717	2. 366993
Au	4. 367527	0. 840531	2. 366993
Au	5. 823370	3. 362125	2. 366993
Au	0. 000000	0. 000000	0. 000000
Au	1. 455843	2. 521594	0. 000000
Au	2. 911685	5. 043187	0. 000000
Au	2. 911685	0. 000000	0. 000000
Au	4. 367527	2. 521594	0. 000000
Au	5. 823370	5. 043187	0. 000000
Au	5. 823370	0. 000000	0. 000000
Au	7. 279213	2. 521594	0. 000000
Au	8. 735055	5. 043187	0. 000000

XYZ format coordinates for Geo. 11:

48

BT/Au111 Geo. 11

C	1. 427023	0. 835287	13. 362285
C	1. 444150	0. 813753	10. 575703
C	0. 220572	0. 827981	12. 655337
C	0. 219814	0. 816530	11. 259890
C	2. 642057	0. 828828	12. 670319

C	2. 660004	0. 817531	11. 274996
H	-0. 729934	0. 830400	13. 194242
H	-0. 718246	0. 809103	10. 698633
H	3. 585868	0. 831860	13. 220914
H	3. 604888	0. 810943	10. 725375
H	1. 420272	0. 844064	14. 454275
S	1. 456048	0. 832010	8. 793631
Au	-0. 144635	-0. 082733	7. 132111
Au	1. 456660	2. 686360	7. 116473
Au	2. 916801	5. 039582	7. 135703
Au	3. 058789	-0. 083550	7. 130434
Au	4. 397068	2. 539729	7. 073653
Au	5. 824298	5. 013067	7. 073183
Au	5. 824420	0. 008593	7. 137298
Au	7. 251223	2. 539947	7. 073566
Au	8. 732137	5. 039474	7. 135849
Au	2. 918450	6. 728941	4. 730779
Au	0. 015958	1. 672855	4. 765087
Au	1. 456520	4. 201386	4. 723540
Au	5. 824058	6. 745527	4. 768819
Au	2. 897121	1. 672792	4. 765215
Au	4. 358670	4. 209696	4. 703969
Au	8. 730309	6. 728533	4. 729741
Au	5. 824068	1. 670957	4. 703792
Au	7. 289482	4. 209714	4. 704031
Au	10. 190896	5. 883717	2. 366993
Au	7. 279211	0. 840531	2. 366993
Au	8. 735053	3. 362125	2. 366993
Au	4. 367527	5. 883717	2. 366993
Au	1. 455842	0. 840531	2. 366993
Au	2. 911685	3. 362125	2. 366993
Au	7. 279212	5. 883717	2. 366993
Au	4. 367527	0. 840531	2. 366993
Au	5. 823370	3. 362125	2. 366993
Au	0. 000000	0. 000000	0. 000000
Au	1. 455843	2. 521594	0. 000000
Au	2. 911685	5. 043187	0. 000000
Au	2. 911685	0. 000000	0. 000000
Au	4. 367527	2. 521594	0. 000000
Au	5. 823370	5. 043187	0. 000000
Au	5. 823370	0. 000000	0. 000000
Au	7. 279213	2. 521594	0. 000000
Au	8. 735055	5. 043187	0. 000000